Int. J. Multiphase Flow Vol. 19, No. 3, pp. 451–470, 1993
Printed in Great Britain. All rights reserved

0301-9322/93 $6.00 + 0.00
Copyright © 1993 Pergamon Press Ltd

AN ANALYTICAL MEANS OF COMPARING THE RATES OF DIFFERENT AGGLOMERATION MECHANISMS, AND ITS APPLICATION TO A PWR CONTAINMENT

J. F. B. PAYNE and G. SKYRME
Nuclear Electric, Berkeley Technology Centre, Berkeley, Gloucs. GL13 9PB, England

(Received 15 January 1990; in revised form 25 March 1993)

Abstract—Agglomeration is an important aspect of aerosol behaviour. Unfortunately, it is described by a non-linear integro-differential equation, for which few analytical solutions are known. The equation can be solved numerically, but this approach has disadvantages. In this paper, agglomeration behaviour is described analytically and this quantitative description is used as a means of comparing the rates of different agglomeration mechanisms. The comparison depends on the average particle size but does not require detailed knowledge of the particle size **distribution**. The method is applied to the agglomeration of an aerosol suspended in the atmosphere of a pressurized water reactor (PWR) containment building. The rate of turbulent agglomeration in the PWR containment depends upon the degree of turbulence at each point in the fluid, expressed as the turbulent energy dissipation rate, ε. An approximate model of the containment flow is solved to obtain a satisfactory estimate of the functions of ε needed in evaluating turbulent agglomeration rates.

Key Words: aerosols, agglomeration, Brownian agglomeration, turbulent agglomeration, gravitational agglomeration, analytical solutions, water reactor containments

1. INTRODUCTION

Agglomeration of aerosol particles causes the size distribution of the particles making up an aerosol to change with time. Most obviously, the size distribution of an aerosol affects the rate of deposition of the aerosol, but it also affects the rate of aerosol heat and mass transfer processes (such as condensation on aerosol particles or removal of atmospheric pollutants). Agglomeration is therefore an important aspect of aerosol behaviour.

Unfortunately, the effect of agglomeration on the size distribution of an aerosol is described by a non-linear integro-differential equation, for which few analytical solutions are known. The equation can be solved numerically, but this approach yields specific answers to specific questions, rather than general answers, which usually come from analytical solutions. Of course, a good understanding is more likely to be obtained from general answers. In this paper, agglomeration behaviour is described analytically (without solving the integro-differential equation completely) and this quantitative description is used as a means of comparing the rates of different agglomeration mechanisms. The different agglomeration mechanisms interact to some extent (Simons *et al.* 1986) but as the object of our paper is to compare the different mechanisms, each is considered separately.

Loss of coolant accidents (LOCAs) in a pressurized water reactor (PWR) could result in the release to the containment of fission products and actinide dust. A large part of this radioactive material would be associated with the aerosol formed from the reactor cooling water. The release of activity to the environment depends upon the time for which the aerosol remains suspended in the containment atmosphere. This time, in turn, depends on the aerosol agglomeration rate, because agglomeration affects the aerosol deposition rate. Hence, aerosol agglomeration could have a strong influence on release of radioactivity to the environment after a LOCA. This paper includes a comparison of the rates at which different agglomeration mechanisms operate in a PWR containment.

The rate of turbulent agglomeration in the PWR containment depends upon the degree of turbulence at each point in the fluid, expressed as the turbulent energy dissipation rate, ε. Evaluation of this parameter requires fairly detailed knowledge of the flow in the containment. A

rigorous solution for the containment flow is well-beyond presently available analytical or computational techniques. Even solutions based on approximate models of turbulence would be very difficult to obtain for the real containment geometry. In this paper, a simple model of the flow in the containment is used to obtain reasonably accurate values of ε in the regions of the containment where ε is expected to be large. This approximate method yields a satisfactory estimate of the functions of ε needed in evaluating turbulent agglomeration rates.

2. AGGLOMERATION RATE PARAMETER, ω

In order to compare agglomeration by different mechanisms, it is necessary to define a suitable parameter which is representative of the agglomeration process whilst being as independent as possible of the system variables. The collision kernel K, is a possible candidate, but since the overall agglomeration rate depends on the number density and size distribution of the aerosol population, it does not give a true measure of the relative agglomeration effectiveness. A better measure (suggested by Longworth in an unpublished note) is the fractional rate of change of the total number of aerosol particles. Here, this measure is termed the agglomeration rate parameter, ω, and is defined as shown below.

The rate at which particle number density is changed by agglomeration is given by

$$-\left(\frac{\mathrm{d}N}{\mathrm{d}t}\right)_{\mathrm{aggl}} = \int_0^\infty n(r_2)\left\{\int_0^{r_2} K(r_1, r_2)n(r_1)\,\mathrm{d}r_1\right\}\mathrm{d}r_2, \qquad [1]$$

where

$n(r)\,\mathrm{d}r$ = number of particles per unit volume with radii between r and $r + \mathrm{d}r$,
$K(r_1, r_2)$ = agglomeration kernel for particles of radii r_1 and r_2

and

N = total number of particles per unit volume.

[It has been assumed that agglomeration occurs at each collision. Pruppacher & Klett (1978) discuss droplet coalescence and conclude that coalescence always occurs when water droplets of radius $\lesssim 350\,\mu$m collide.]

The particle size distribution $n(r)\,\mathrm{d}r$ may be written in terms of a dimensionless particle radius R and a normalized size distribution $f(R)$ as follows:

$$n(r)\,\mathrm{d}r = Nf(R)\,\mathrm{d}R, \qquad [2]$$

where

$$R = \frac{r}{r_c}$$

and

r_c = some characteristic particle size for the distribution.

From the definition of N,

$$\int_0^\infty f(R)\,\mathrm{d}R = 1. \qquad [3]$$

When $K(r_1, r_2)$ is a homogeneous function of the particle radii of degree q then, by definition,

$$K(r_1, r_2) = r_c^q K(R_1, R_2). \qquad [4]$$

The volume fraction of particles, ϕ, is the fraction of a given volume that is occupied by particles, hence

$$\phi = \tfrac{4}{3}\pi \int_0^\infty r^3 n(r)\,\mathrm{d}r = \tfrac{4}{3}\pi N r_c^3 \int_0^\infty R^3 f(R)\,\mathrm{d}R. \qquad [5]$$

Using [3]–[5] in [1], the agglomeration rate may be written as

$$-\left(\frac{dN}{dt}\right)_{aggl} = \omega N,$$

where

$$\omega = \frac{3\phi}{4\pi} r_c^{q-3} \frac{\int_0^\infty f(R_2)\left\{\int_0^{R_2} K(R_1, R_2) f(R_1)\, dR_1\right\} dR_2}{\int_0^\infty R^3 f(R)\, dR} \qquad [6]$$

is the agglomeration rate parameter.

The agglomeration rate parameter, ω, is not, in general, a constant since $f(R)$ varies as agglomeration proceeds (and ϕ also changes if there is particle deposition or a particle source). Furthermore, except for special cases where $q = 3$, increases in r_c also affect ω. However, since ω is proportional to the particle volume fraction, ϕ, for all agglomeration mechanisms, the variation of ω/ϕ with r_c provides a useful method of comparing the different mechanisms.

3. BROWNIAN AGGLOMERATION

In general the Brownian collision kernel is a function of the gas mean-free-path, but for particles whose radii are much larger than the mean-free-path (0.06 μm for air at NTP) the dependence is negligible. In this case, within Smoluchowski's approximation, the collision kernel for Brownian agglomeration, K_B, is independent of particle size, and is given by

$$K_B = \frac{8kT}{3\mu}, \qquad [7]$$

where

k = Boltzmann's constant,
T = absolute temperature

and

μ = gas dynamic viscosity.

Hence $K_B(R_1, R_2) = K_B(r_1, r_2)$ and $q = 0$.

The equation defining ω contains $f(R)$, which is unknown. This difficulty can be circumvented by choosing the characteristic radius of the particle size distribution, r_c, to be the volume mean radius, r_v, defined by

$$\tfrac{4}{3}\pi r_v^3 N = \phi = \int_0^\infty \tfrac{4}{3}\pi r^3 n(r)\, dr,$$

which implies (cf. [5]) that

$$\int_0^\infty R^3 f(R)\, dR = 1. \qquad [8]$$

Using [3], [7] and [8], [6] gives the Brownian rate parameter ω_B as

$$\omega_B = \frac{\phi kT}{\pi \mu r_v^3}, \qquad [9]$$

which only depends on the particle size distribution to the extent that it affects the volume mean particle radius.

In the case of turbulent or gravitational agglomeration, it is not so easy to avoid specifying the particle size distribution. However, since Brownian agglomeration predominates for small particle sizes, it will be the mechanism that increases particle size to the point where other agglomeration mechanisms become important. Friedlander & Wang (1966) have shown that Brownian

agglomeration causes any particle size distribution to asymptotically approach the form

$$n^*(V, t)\,\mathrm{d}V = \frac{N(t)^2}{\phi}\exp\left(-\frac{N(t)V}{\phi}\right)\mathrm{d}V, \qquad [10]$$

where $n^*(V, t)\,\mathrm{d}V$ is the number of particles per unit volume with volume between V and $V + \mathrm{d}V$. It is therefore reasonable to assume that this will be a good approximation to the size distribution, when turbulent and gravitational agglomeration first become significant. The size distribution as a function of volume can be transformed to a size distribution as a function of radius, as shown in appendix A. The result is

$$n(r)\,\mathrm{d}r = Nf_B(R)\,\mathrm{d}R = N\exp(-R^3)3R^2\,\mathrm{d}R, \qquad [11]$$

where the characteristic radius is again the volume mean radius, r_v.

4. GRAVITATIONAL AGGLOMERATION

Differences in the gravitational settling velocities of particles in a population due to differences in density, size or shape can result in collisions which give rise to gravitational agglomeration. The collision kernel, $K_G(r_1, r_2)$, is given by

$$K_G(r_1, r_2) = \pi(r_1 + r_2)^2[u(r_1) - u(r_2)]E(r_1, r_2),$$

where

$u(r)$ = terminal settling velocity of particles of radius r

and

$E(r_1, r_2)$ = collision efficiency for particles of radius r_1 and r_2.

For water droplets in air which are large compared with the mean-free-path of the gas molecules (0.06 μm) and whose radii are less than $\sim 30\,\mu$m, $u(r)$ is adequately given by the Stokes equation

$$u(r) = \frac{2\rho g}{9\mu}r^2, \qquad [12]$$

where

$\rho = \rho_p - \rho_f$,
ρ_p = particle density
ρ_f = fluid density

and

g = acceleration due to gravity

The central problem in gravitational agglomeration is the evaluation of the collision efficiency, E. No attempt to review this topic has been made by the authors. However, E has been discussed by Dunbar & Ramsdale (1984), and for particle radii $< 10\,\mu$m they recommend the use of the "truncated" Pruppacher & Klett (1978) equation:

$$E(r_1, r_2) = \begin{cases} \frac{1}{2}\left(\frac{r_1}{r_1 + r_2}\right)^2 & \text{for } \frac{r_1}{r_2} < 0.5 \\ 0.05 & \text{for } 0.5 \leqslant \frac{r_1}{r_2} \leqslant 1.0. \end{cases}$$

[These equations introduce a physically unrealistic discontinuity at $r_1/r_2 = 0.5$. To avoid this, in carrying out the computations $E(r_1, r_2)$ was calculated from both equations and the lower value of E was used.]

Thus in terms of the dimensionless particle radii the gravitational collision kernel is given by

$$K_G(r_1, r_2) = r_c^4 K_G(R_1, R_2),$$

where

$$K_G(R_1, R_2) = \pi \frac{2\rho g}{9\mu} (R_1 + R_2)^3 (R_1 - R_2) E(R_1, R_2). \quad [13]$$

Hence $q = 4$.

Since the collision kernel is a strong function of the particle sizes, the choice of the particle size distribution is very important. Provided the particles are small initially, the distribution will evolve to that resulting from Brownian agglomeration (as given by [11]) by the time that the particles are large enough for gravitational agglomeration to be important. As gravitational agglomeration proceeds, however, the distribution will change. In order to estimate the effect of changes in the distribution, therefore, a log-normal distribution will also be considered.

4.1. Brownian Size Distribution

Substituting [11] and [13] into [6], and noting that the characteristic radius, r_c, is r_v, the initial gravitational agglomeration rate parameter, $\omega_G(0)$, is given by

$$\omega_G(0) = \frac{3\phi}{4\pi} \frac{2\rho g \pi}{9\mu} \times \frac{r_v \int_0^\infty 3 \exp(-R_2^3) R_2^2 \left\{ \int_0^{R_2} (R_1 + R_2)^3 (R_2 - R_1) E(R_1, R_2) 3 \exp(-R_1^3) R_1^2 \, dR_1 \right\} dR_2}{\int_0^\infty 3 \exp(-R^2) R^5 \, dR}. \quad [14]$$

It follows from the definition of r_v that the denominator in the above equation is unity. The double integral in the numerator has to be evaluated numerically. The value of the integral, accurate to better than four significant figures, is 5.865×10^{-2}. Thus,

$$\omega_G(0) = \frac{\phi}{6} \frac{\rho g}{\mu} r_v 5.865 \times 10^{-2}. \quad [15]$$

4.2. Log-normal Size Distribution

The dimensionless particle distribution function corresponding to a log-normal size distribution is

$$f_l(R) \, dR = \frac{1}{\sqrt{2\pi} \ln \beta_g} \exp\left\{ -\frac{1}{2} \left(\frac{\ln R}{\ln \beta_g} \right)^2 \right\} \frac{dR}{R}, \quad [16]$$

where

$$R = \frac{r}{r_g},$$

r_g = geometric mean of the particle radii

and

β_g = standard geometric deviation.

Thus, substituting [13] and [16] into [6], and noting that the characteristic radius, r_c, is now r_g, the gravitational agglomeration rate parameter for the log-normal size distribution, $\omega_G(l)$, is

$$\omega_G(l) = \frac{3\phi}{4\pi} \frac{2\rho g \pi}{9\mu} r_g \frac{\Psi}{\Theta}, \quad [17]$$

where

$$\Psi = \frac{1}{2\pi (\ln \beta_g)^2} \int_0^\infty \int_0^{R_2} \frac{(R_1 + R_2)^3 (R_2 - R_1) E(R_1, R_2)}{R_1} \exp\left\{ -\frac{1}{2} \left(\frac{\ln R_1}{\ln \beta_g} \right)^2 \right\} dR_1 \times \exp\left\{ -\frac{1}{2} \left(\frac{\ln R_2}{\ln \beta_g} \right)^2 \right\} \frac{dR_2}{R_2}$$

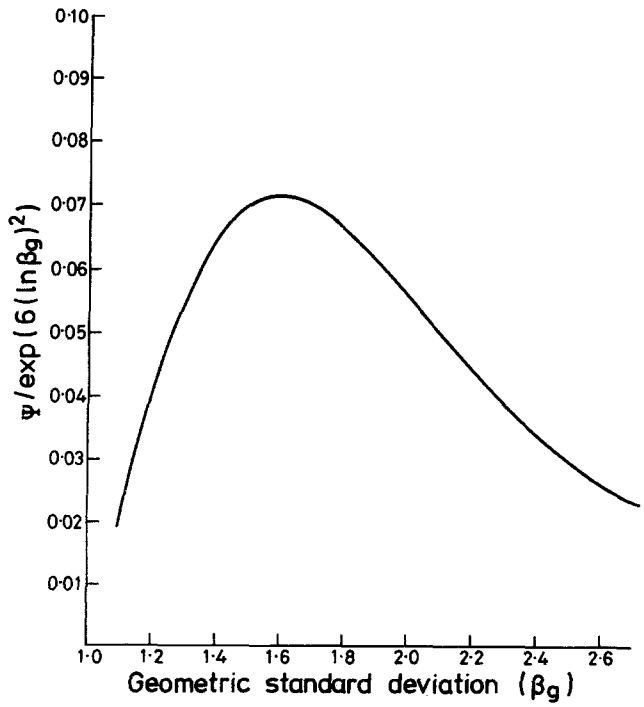

Figure 1

and

$$\Theta = \frac{1}{\sqrt{2\pi}\ln\beta_g}\int_0^\infty \exp\left\{-\frac{1}{2}\left(\frac{\ln R}{\ln\beta_g}\right)^2\right\} R^2\,dR = \exp\{\tfrac{9}{2}(\ln\beta_g)^2\}.$$

Noting that, for a log-normal distribution,

$$r_v = r_g \exp\{\tfrac{3}{2}(\ln\beta_g)^2\},$$

[17] becomes

$$\omega_G(l) = \frac{\phi}{6}\frac{\rho g}{\mu} r_v \frac{\Psi}{\exp\{6(\ln\beta_g)^2\}}.$$

The integral Ψ has been evaluated numerically, and values of $\Psi/\exp\{6(\ln\beta_g)^2\}$ as a function of β_g are shown in figure 1. For typical values of β_g (1.1–2.5) the function is relatively insensitive to β_g and has the value $\sim 0.05 \pm 0.02$. Size distributions outside this range will have smaller agglomeration parameters. Thus,

$$\omega_G(l) \simeq \frac{\phi}{6}\frac{\rho g}{\mu} r_v (0.05 \pm 0.02). \qquad [18]$$

5. TURBULENT AGGLOMERATION

Saffman & Turner (1956) presented a paper on the agglomeration of particles caused by turbulence of the suspending fluid. The paper has been quoted extensively in subsequent treatises on turbulent agglomeration and forms the basis of most computer codes on this subject. A brief description of the theory is given here together with the relevant equations.

The theory applies to particles that are much smaller than the small eddies of the turbulence, so that the relative motion of the particles is governed by the small eddies. Eddies are associated with deformation and acceleration of the fluid. These two processes give rise to the two

agglomeration mechanisms described by Saffman & Turner (1956). The first mechanism is caused by the motion of the fluid itself, whereas the second is caused by motion of the particle relative to the fluid.

Within a small region, the motions of the fluid, relative to a point moving with the fluid, may be resolved into a strain and a rotation. Clearly, rotation of the fluid does not affect the distance between particles moving with it. Strain, on the other hand, causes an initially spherical region of the fluid to become ellipsoidal in shape. Thus, particles in some parts of the initially spherical region will be brought closer together and may undergo collisions and agglomerate. The term "turbulent strain agglomeration" may be used for this mechanism of agglomeration due to motion with the fluid. A shear motion has a non-zero strain component and therefore can cause agglomeration. Hence the mechanism is sometimes referred to as turbulent shear agglomeration.

Acceleration of the fluid will cause suspended particles to move relative to the fluid (because of their inertia). The relative velocity between particle and fluid caused by acceleration will be different for particles of different mass or size, just as particles have different settling velocities under gravity (a constant acceleration is indistinguishable from gravity in its effects). Although the fluid accelerations are not constant, it will be a good approximation to treat them as constant provided that the time scale of fluctuations in fluid acceleration is long compared to the particle relaxation time, $\tau = 2r^2\rho_p/9\mu$. This is a necessary condition for the validity of Saffman & Turner's (1956) calculations of agglomeration "due to motion relative to the air". This agglomeration mechanism, resulting from the different relative particle velocities induced by the fluid acceleration, is commonly referred to as turbulent inertial agglomeration.

Saffman & Turner (1956) assumed that the collision efficiency for both strain and inertial mechanisms is unity, citing experimental evidence on shear agglomeration to justify the assumption. This assumption was made "in the absence of further evidence". Since their paper appeared, the collision efficiency of particles falling under gravity has been investigated experimentally and theoretically, and better approximations than collision efficiency $\simeq 1$ are available. However, later experimental evidence (Okuyama *et al.* 1978) is consistent with a collision efficiency of 1 for strain agglomeration. In this paper, therefore, the collision efficiency will be taken to be 1 for strain agglomeration, but for the inertial mechanism the Pruppacher and Klett equations for the gravitational collision efficiency will be used.

A detailed discussion of strain agglomeration is given by Payne (1988), who shows that, although Saffman & Turner's (1956) paper has a typographical error, the final result is correct (Saffman 1988). The collision kernel for turbulent strain agglomeration is

$$K_{Ts}(r_1, r_2) = (r_1 + r_2)^3 \sqrt{\frac{8\pi\varepsilon}{15\nu}}, \qquad [19]$$

where

ε = turbulent energy dissipation rate per unit mass of fluid

and

$\nu = \dfrac{\mu}{\rho_f}$ is the kinematic viscosity.

Calculation of the inertial term is more difficult, and Saffman & Turner (1956) derived only an approximate expression for the collision rate, by assuming a simple, idealized form for the probability distribution, $P(\mathbf{w})$, of the particles' relative velocity $\mathbf{w}$. $P(\mathbf{w})$ was chosen such that the resulting variance in $\mathbf{w}$ was equal to the variance calculated from the relative **fluid–fluid** velocity (equivalent to the strain term above) and the relative **fluid–particle** velocity. The latter, which is calculated from the equation of motion of the particle, gives the inertial component of agglomeration and includes the effect of gravity. The resultant collision kernel is

$$(r_1 + r_2)^2 \sqrt{\frac{8\pi}{3}\left(\frac{2\rho}{9\mu}\right)^2 (r_1^2 - r_2^2)^2 \left[\left(\frac{\mathrm{D}\mathbf{u}}{\mathrm{D}t}\right)^2 + g^2\right] + \frac{8\pi}{9}(r_2 + r_2)^2 \frac{\varepsilon}{\nu}},$$

where **u** is the velocity of the fluid surrounding the particle and D/Dt denotes differentiation following the fluid. The terms in square brackets represent the effect of fluid acceleration and gravity, and the term involving ε represents the effect of fluid strain. Comparison of the gravitational term with [13] shows that, apart from the collision efficiency, the two only differ by a small numerical factor π, cf. $\sqrt{8\pi/3}$. Similarly, the strain component only differs by a small factor $\sqrt{8\pi/9}$, compared to, $\sqrt{8\pi/15}$ [19].

The good agreement between these two terms and the rigorous solutions gives confidence that the inertial term, too, is correct to within a factor of ~ 2.

The most cogent argument in favour of the inclusion of the inertial term, however, is that turbulent acceleration is, in principle, indistinguishable from gravity (except that it is unsteady), and so the gravitational agglomeration expressions must apply, but with g replaced by turbulent acceleration.

Noting that the turbulent acceleration is given by (Batchelor 1951).

$$\overline{\left(\frac{\mathrm{D}\mathbf{u}}{\mathrm{D}t}\right)^2} = 3 \times 1.3 \frac{\varepsilon^{3/2}}{\nu^{1/2}}$$

and including the collision efficiency, the inertial turbulent collision kernel, $K_{\mathrm{Ti}}(r_1, r_2)$, becomes

$$K_{\mathrm{Ti}}(r_1, r_2) = \pi \frac{2\rho}{9\mu} (r_1 + r_2)^3 (r_1 - r_2) \sqrt{\frac{8 \times 1.3\varepsilon^{3/2}}{\pi \nu^{1/2}}} E(r_1, r_2).$$

Thus, in terms of the dimensionless particle radii, the turbulent strain collision kernel is given by

$$K_{\mathrm{Ts}}(r_1, r_2) = r_c^3 K_{\mathrm{Ts}}(R_1, R_2),$$

where

$$K_{\mathrm{Ts}}(R_1, R_2) = (R_1 + R_2)^3 \sqrt{\frac{8\pi\varepsilon}{15\nu}}. \qquad [20]$$

The turbulent inertial collision kernel is

$$K_{\mathrm{Ti}}(r_1, r_2) = r_c^4 K_{\mathrm{Ti}}(R_1, R_2),$$

where

$$K_{\mathrm{Ti}}(R_1, R_2) = \pi \frac{2\rho}{9\mu} \sqrt{\frac{8 \times 1.3\varepsilon^{3/2}}{\pi \nu^{1/2}}} (R_1 + R_2)^3 (R_1 - R_2) E(R_1, R_2). \qquad [21]$$

Doubt has been expressed about whether the inertial term should be included in turbulent agglomeration since, it is suggested, the experiments of Delichatsios & Probstein (1975) and Okuyama *et al.* (1978) may be explained in terms of strain agglomeration only. The ratio of the inertial to the strain agglomeration rate is

$$\frac{K_{\mathrm{Ti}}(r_1, r_2)}{K_{\mathrm{Ts}}(r_1, r_2)} \simeq (R_1 - R_2) E(R_1, R_2) r_c \frac{\rho}{\mu} (\varepsilon\nu)^{1/4}.$$

Thus, the strain dominates over the inertial mechanism at low turbulent energy dissipation rates, for high viscosity fluids and when the particle/fluid density difference is small. Under the conditions in Delichatsios & Probstein's (1975) experiment (0.6 μm latex spheres in water with $\varepsilon \simeq 0.3\ \mathrm{m^2\,s^{-3}}$), the inertial mechanism would not be expected to be significant; and in the Okuyama *et al.* (1978) experiments (0.27–0.9 μm liquid droplets in air with ε from 8 to $8 \times 10^3\ \mathrm{m^2\,s^{-3}}$), the authors themselves consider that the inertial mechanism causes the departure of their data from the strain equation with increasing intensity of turbulence and at larger particle sizes.

There seems little justification, either on theoretical or experimental grounds, for discarding the inertial term, and it is recommended that it be retained in agglomeration calculations.

6. TURBULENT AGGLOMERATION PARAMETER

The equations discussed in section 5 will be used to evaluate the agglomeration parameter ω_{T} for two particle size distributions. For the reasons already discussed in section 4, ω_{T} will be

evaluated both for the particle size resulting from Brownian agglomeration and for a log-normal distribution. The inertial and strain mechanisms will be evaluated separately.

6.1. *Turbulent Strain Agglomeration*

Substituting [20] into [6] and noting that for this case $q = 3$, the turbulent strain agglomeration parameter becomes

$$\omega_{Ts} = \frac{\frac{3\phi}{4\pi}\sqrt{\frac{8\pi\varepsilon}{15\nu}}\int_0^\infty f(R_2)\left\{\frac{1}{2}\int_0^\infty (R_1+R_2)^3 f(R_1)\,dR_1\right\}dR_2}{\int_0^\infty R^3 f(R)\,dR}. \quad [22]$$

Expanding $(R_1 + R_2)^3$ in [22], the integrals over R_1 and R_2 can be separated, so that

$$\omega_{Ts} = \frac{\frac{3\phi}{4\pi}\sqrt{\frac{8\pi\varepsilon}{15\nu}}\left\{\int_0^\infty f(R)\,dR\int_0^\infty R^3 f(R)\,dR + 3\int_0^\infty Rf(R)\,dR\int_0^\infty R^2 f(R)\,dR\right\}}{\int_0^\infty R^3 f(R)\,dR}. \quad [23]$$

6.1.1. *Brownian size distribution*

Substituting [11] into [23] and noting that (Abramowitz & Stegun 1965)

$$\int_0^\infty R^a f_B(R)\,dR = \Gamma\left(1+\frac{a}{3}\right),$$

$$\Gamma(2) = \Gamma(1) = 1$$

and

$$\Gamma\left(\frac{4}{3}\right)\Gamma\left(\frac{5}{3}\right) = \frac{1}{3}\Gamma\left(\frac{1}{3}\right)\frac{2}{3}\Gamma\left(\frac{2}{3}\right) = \frac{1}{3}\frac{2}{3}\frac{2\pi}{\sqrt{3}},$$

the turbulent strain agglomeration parameter for a Brownian distribution is given by

$$\omega_{Ts}(0) = \frac{3\phi}{4\pi}\sqrt{\frac{8\pi\varepsilon}{15\nu}}\left(1+\frac{4\pi}{3\sqrt{3}}\right). \quad [24]$$

6.1.2. *Log-normal size distribution*

Substituting [16] into [23] and noting that (Aitchison & Brown 1973)

$$\int_0^\infty R^a f_l(R)\,dR = \exp\left\{\frac{a^2}{2}(\ln\beta_g)^2\right\},$$

the turbulent strain agglomeration parameter for a log-normal distribution becomes

$$\omega_{Ts}(l) = \frac{3\phi}{4\pi}\sqrt{\frac{8\pi\varepsilon}{15\nu}}\,(1+3\exp\{-2(\ln\beta_g)^2\}). \quad [25]$$

The function $(1 + 3\exp\{-2(\ln\beta_g)^2\})$ is shown in figure 2. The function varies quite rapidly, but is bounded by the upper limit of 4 and the lower limit of 1 (indeed, these bounds apply for an arbitrary size distribution). However, over the range of β_g that is likely to occur in practice, the function may be approximated by $\sim 2.5 \pm 1$. Thus,

$$\omega_{Ts}(l) \simeq \frac{3\phi}{4\pi}\sqrt{\frac{8\pi\varepsilon}{15\nu}}\,(2.5\pm 1). \quad [26]$$

6.2. *Turbulent Inertial Agglomeration*

As discussed in section 5, turbulent inertial agglomeration arises from the response of particles to the acceleration of the fluid. Therefore, the form of the collision kernel, [21], is similar to that for gravitational agglomeration, [13], with the acceleration due to gravity, g, replaced by a turbulent

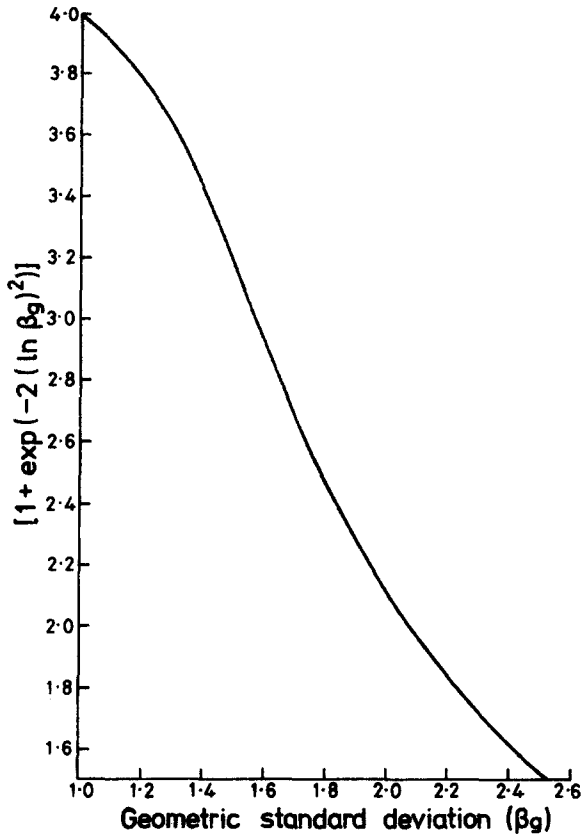

Figure 2

acceleration, g_T, given by

$$g_T = \sqrt{\frac{8 \times 1.3\varepsilon^{3/2}}{\pi \nu^{1/2}}}. \qquad [27]$$

Thus, the inertial agglomeration rate parameters for the two particle size distributions may be deduced from the results of section 4.

6.2.1. Brownian size distribution

Replacement of g in [15] by g_T and use of [27] yields

$$\omega_{Ti}(0) = \frac{\phi}{6}\frac{\rho}{\mu} r_v \sqrt{\frac{8 \times 1.3\varepsilon^{3/2}}{\pi \nu^{1/2}}}\, 5.865 \times 10^{-2}. \qquad [28]$$

6.2.2. Log-normal size distribution

Replacement of g in [19] by g_T and use of [27] yields

$$\omega_{Ti}(l) \simeq \frac{\phi}{6}\frac{\rho}{\mu} r_v \sqrt{\frac{8 \times 1.3\varepsilon^{3/2}}{\pi \nu^{1/2}}}\,(0.05 \pm 0.02). \qquad [29]$$

7. TURBULENT ENERGY DISSIPATION RATE, ε

In order to calculate the agglomeration rate due to turbulence in the fluid it is necessary to know the turbulent energy dissipation rate, ε, which is the rate of dissipation of fluid kinetic energy per unit mass of fluid. Following the release of radioactivity to the PWR containment there will be several sources of energy input to the containment. Not all of this energy will be dissipated by fluid motion, however, since much will be lost by conduction, condensation, radiation etc. In order to

calculate ε, therefore, it is necessary to have a detailed description of the flow generated by these energy sources.

A further, major complication arises due to the fact that it is not ε^1 but $\varepsilon^{1/2}$ or $\varepsilon^{3/4}$ which appears in the agglomeration rate parameter. Thus, for a uniform spacial particle distribution, it is the average value (denoted by an overbar) of $\varepsilon^{1/2}$ or $\varepsilon^{3/4}$ that is required, rather than $\bar{\varepsilon}$. When the energy dissipation is uniformly distributed throughout the containment this causes no problem. If only a small fraction, f, of the volume is involved, however, there can be a substantial difference between $\bar{\varepsilon}^{1/2}$ and $\overline{\varepsilon^{1/2}}$, since

$$\overline{\varepsilon^{1/2}} = f^{1/2}\bar{\varepsilon}^{1/2}.$$

In the case of a steam jet, for example, the volume in which the turbulent energy is dissipated may be only $\sim 10^{-4}$ of the containment volume, in which case

$$\overline{\varepsilon^{1/2}} = 10^{-2}\bar{\varepsilon}^{1/2},$$

i.e. two orders of magnitude difference.

Thus, it is essential to know the **distribution** of the energy dissipation, and this imposes a further requirement for a specific model of the turbulent energy dissipation mechanism. The complicated geometry of the containment, the existence of several sources of fluid kinetic energy, and the diversity of the accident sequences, preclude a general solution to the problem. In the following sections, the turbulent dissipation of energy from several different possible sources is estimated.

In principle, thermal hydraulic computer codes can be used to model specific accidents and give values for $\overline{\varepsilon^{1/2}}$ and $\overline{\varepsilon^{3/4}}$. A particular case of a buoyant steam jet in a containment (the LACE experiment) has been analysed using the FEAT fluid mechanics code (Hutton in an unpublished work). The results obtained support the simpler method of calculation used in sections 7.1 (for a steam plume) and 7.3 (for a jet).

7.1. Steam Plume

The major energy input mechanism to the containment atmosphere is believed to be the steam plume, issuing from a breach in the primary circuit, produced by boiling of the reactor coolant by the decay heat. In this section, a simplified model of this situation is analysed to estimate $\overline{\varepsilon^{1/2}}$ and $\overline{\varepsilon^{3/4}}$. Three cases will be considered:

1. 40 MW decay heat, steam emerging at 100°C through a 1 m dia hole into a containment at 1 bar and 40°C.
2. 40 MW decay heat, steam emerging at 100°C through four well-separated 1 m dia holes into a containment at 1 bar and 40°C.
3. 20 MW decay heat, steam emerging at 145°C through a 1 m dia hole into containment at 4 bar and 145°C.

The components of the plume energy which are dissipated as turbulence in the containment are the kinetic energy, and the gravitational potential energy of the buoyant steam. Thus, case 1 corresponds to a relatively high turbulent energy dissipation rate, since the decay heat (and hence steam flow rate) is high. Also, the density difference between the plume and the containment atmosphere (and hence the buoyancy) is large. Case 2 corresponds to a leak into an internal compartment, such that the steam emerges into the open containment through four holes. In this case the spatial distribution of the dissipation of gravitational potential energy is more even, but the kinetic energy is almost all dissipated in the internal compartment, making a negligible contribution to the containment-averaged $\varepsilon^{1/2}$ or $\varepsilon^{3/4}$. Case 3 is intended to represent the low end of the range of possible accidents. It has a lower steam flow rate and, at the higher containment pressure, the density difference between the plume and the atmosphere is less than in cases 1 and 2.

Details of the analysis of steam plume behaviour are given in appendix B. The results of the analysis show that buoyancy is the major contributor to $\overline{\varepsilon^{1/2}}$, since the plume rises to the full 50 m containment height driven by the buoyancy (the plume radius at 50 m was ~ 10 m), whereas the kinetic energy is dissipated over a short plume length.

The values obtained for $\overline{\varepsilon^{1/2}}$ and $\overline{\varepsilon^{3/4}}$ for the three cases are:

	case 1	case 2	case 3
$\overline{\varepsilon^{1/2}}$ $(m^2 s^{-3})^{1/2}$	~0.08	~0.1	~0.01
$\overline{\varepsilon^{3/4}}$ $(m^2 s^{-3})^{3/4}$	~0.1	~0.08	~0.004

The values for cases 1 and 2 are similar because the more even distribution of potential energy dissipation approximately compensates for the loss of the kinetic energy contribution. $\overline{\varepsilon^{1/2}}$ is more sensitive to the distribution of ε than $\overline{\varepsilon^{3/4}}$, hence case 2 gives a slightly higher value of $\overline{\varepsilon^{1/2}}$ than case 1 but a slightly lower value of $\overline{\varepsilon^{3/4}}$.

7.2. Sprays

Operation of the spray in the containment following a release of steam will result in a recirculating air flow, downwards in the centre and upwards near the containment walls. Turbulent energy will be dissipated in this flow. Measurements at the Ringhals LWR showed that the maximum entrained air velocity was 4.5 m s^{-1}, with a representative value of about 1–2 m s^{-1}. Similar values may be assumed for Sizewell, and used to estimate the turbulent energy dissipation rate. Townsend (1976), for example, shows that

$$\varepsilon \simeq \frac{u'^3}{l},$$

where

u' = fluctuating component of the flow velocity

and

l = dimension of the large eddies.

Typically, u' may be up to 1/10 of the mainstream flow velocity (Bradshaw 1971). Taking l to be 1/10 of the containment dimension of ~50 m,

$$\varepsilon \simeq \frac{(0.2)^3}{5} = 0.0016 \text{ m}^2 \text{ s}^{-3}.$$

In this case the flow is likely to be distributed relatively uniformly over the containment volume so that

$$\overline{\varepsilon^{1/2}} \simeq \bar{\varepsilon}^{1/2} \simeq 0.04 \text{ } (\text{m}^2 \text{ s}^{-3})^{1/2}$$

and

$$\overline{\varepsilon^{3/4}} \simeq \bar{\varepsilon}^{3/4} \simeq 0.008 \text{ } (\text{m}^2 \text{ s}^{-3})^{3/4}.$$

7.3. Hydrogen Mixing Fans

The hydrogen mixing fans are designed to produce jets that reach the containment roof, in order to keep the atmosphere well-mixed and prevent the local accumulation of explosive concentrations of hydrogen. These fans will contribute to the turbulence in the containment. There are four fans, each with a flow rate of 20 m^3 s^{-1}, and a discharge area of ~1.8 m^2. Regarding the flow from each fan as an air jet with initial velocity of 11 m s^{-1} and no buoyancy, then following the method of calculation in appendix B the mean turbulent energy dissipation rates generated by all four fans are:

$$\overline{\varepsilon^{1/2}} = 0.06 \text{ } (\text{m}^2 \text{ s}^{-3})^{1/2}$$

and

$$\overline{\varepsilon^{3/4}} = 0.05 \text{ } (\text{m}^2 \text{ s}^{-3})^{3/4}.$$

Although these dissipation rates are smaller than those of cases 1 and 2 for the steam jet, they are far from negligible and have the advantage that they are less dependent on the details of the accident. (In certain accidents not all four fans may be working.)

7.4. Containment Fan Coolers

The fans that circulate the containment atmosphere through the four coolers are a further source of turbulent energy. During a LOCA, the flow rate through each cooler is 32 $m^3 s^{-1}$ (Gittus *et al.* 1984). In normal operation the fans blow air through ducting, but during a LOCA fusible links melt and allow a direct path to the containment to open. The flow area into the containment approximately equals the cross-sectional area of the fan (Sizewell B Pre-Construction Safety Report 1982). The fan tip diameter is 66″ (Gittus *et al.* 1984). Thus, the fan coolers produce a jet of velocity ~ 14 m s^{-1} from an area of ~ 2.2 m^2. These figures correspond to a kinetic energy flux about 3 times larger than that produced by the hydrogen mixing fans, so larger values of ε might be expected. However, the containment cooler fans exhaust close to the wall of the containment where there are several structures, so it is not realistic to treat the flows as free jets. Detailed modelling of the containment geometry, in the fan exhaust region at least, would be necessary to estimate the distribution of ε. Qualitatively, interaction of the jets with walls and other structures causes localized dissipation of energy, compared to a free jet. Therefore, despite the increase in kinetic energy flux, it is unlikely that the fan coolers produce significantly larger values of $\overline{\varepsilon^{1/2}}$ or $\overline{\varepsilon^{3/4}}$ than the hydrogen mixing fans.

8. NUMERICAL VALUES OF THE AGGLOMERATION RATE PARAMETER IN A PWR

In order to compare the agglomeration rate parameters for the various mechanisms discussed above it is necessary to assign numerical values to the parameters in the equations. A saturated steam/air mixture at 100°C is assumed, and the following values are used:

$$k = 1.38 \times 10^{-23}\ \mathrm{J\,K^{-1}},$$

$$T = 100°\mathrm{C}\ (373\ \mathrm{K}),$$

$$\mu = 2 \times 10^{-5}\ \mathrm{kg\,m^{-1}\,s^{-1}},$$

$$\rho = (\rho_p - \rho_f) = 1 \times 10^{3}\ \mathrm{kg\,m^{-3}},$$

$$g = 9.8\ \mathrm{m\,s^{-2}}$$

and

$$\nu = 1 \times 10^{-5}\ \mathrm{m^2\,s^{-1}}.$$

The consideration of the turbulent energy dissipation rate in section 7 showed that the steam jet is likely to be the major contributor to the relevant turbulent energy parameters, $\overline{\varepsilon^{1/2}}$ and $\overline{\varepsilon^{3/4}}$. Values quoted in that section are only approximate, and depend on the specific details of the incident. In evaluating the importance of turbulent agglomeration, it is sufficient to use the highest values from the three cases considered. These values are $\overline{\varepsilon^{1/2}} = 0.1\ (\mathrm{m^2\,s^{-3}})^{1/2}$ and $\overline{\varepsilon^{3/4}} = 0.1\ (\mathrm{m^2\,s^{-3}})^{3/4}$.

Using these values, ω/ϕ (agglomeration rate parameter divided by particle volume fraction) has been calculated for the various agglomeration mechanisms. The results are shown in figure 3. (For gravitational and turbulent inertial agglomeration, the ω/ϕ curves for the log–normal and [11] particle size distributions are virtually identical, so only one line is shown.)

9. DISCUSSION

Brownian agglomeration is well-understood for particles larger than the mean-free-path of the gas molecules, as is the case here, and, since the rate parameter is insensitive to the size distribution when the volume mean radius is used, [12] and the line shown in figure 3 may be taken as well-established.

The gravitational agglomeration rate constant is strongly dependent on the collision efficiency and no attempt has been made in this paper to assess this parameter. The value used was that recommended by Dunbar & Ramsdale (1984). The particle size distribution strongly affects the gravitational agglomeration rate. If the aerosol droplets are small initially, then, when gravitational

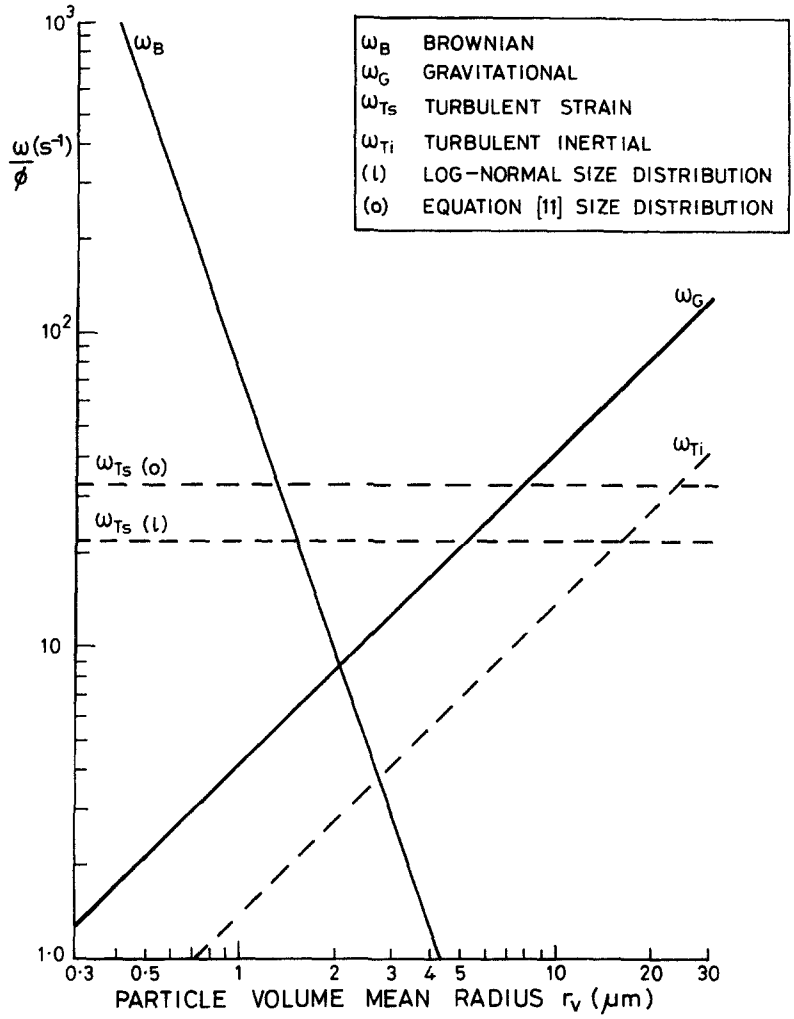

Figure 3

agglomeration first becomes significant, the size distribution is that resulting from Brownian agglomeration. As agglomeration proceeds the distribution may change; to assess this the rate parameter for a log-normal as well as a Brownian distribution was calculated. Over the range of log-normal distributions likely to be encountered in practice ω_G only varied by $\sim \pm 50\%$, the average being close to that for the Brownian distribution. Only in the unlikely cases of an extremely wide or an almost monodisperse distribution will the rate parameter differ significantly from that shown in figure 3.

The Saffman & Turner (1956) theory of turbulent agglomeration has been discussed. Whilst it is recognized that their treatment of inertial agglomeration is only approximate (compared to that of strain agglomeration, which is relatively rigorous), there seems little doubt that the phenomenon exists, and that their equations are probably correct to within a factor of 2. Furthermore, there is no justification on the experimental evidence to ignore the inertial term. Therefore, it is recommended that the term be retained in agglomeration calculations.

The collision efficiency in turbulent agglomeration is not well-established. Since the strain and inertial mechanisms are quite different there is no reason for the collision efficiencies to be the same for each. Saffman & Turner (1956) cited evidence suggesting a value of unity for the strain agglomeration efficiency, and this is supported by later experiments (Okuyama *et al.* 1978) so unit strain agglomeration efficiency has been used here. The equivalence of the inertial mechanism to gravitational agglomeration suggests that the same collision efficiency be used in both cases, and

this is done here. (This also ensures a degree of consistency when comparing the gravitational and inertial mechanisms.)

The sensitivity of the turbulent agglomeration rate parameters to the particle size distribution has been evaluated. For the inertial mechanism, the sensitivity is the same as for gravitational agglomeration, i.e. $\sim \pm 50\%$. For the strain mechanism also the uncertainty is unlikely to be $> \pm 50\%$.

The greatest uncertainty in turbulent agglomeration is in the turbulent energy dissipation rate, ε, largely because account must be taken of its spacial variation when calculating the appropriate quantities to be used in the agglomeration equations. These quantities depend on the flow in the containment and, hence, are strongly sensitive to the details of the accident and the containment geometry. Computational fluid mechanics codes may provide accurate values for reasonably simple geometries, but these are not presently available for even a simplified PWR containment geometry. Furthermore, it would be very difficult to obtain solutions in the real containment geometry (including internal structures, for instance). Therefore, estimates have been made of the turbulent energy dissipation rate from a selection of sources, using a very simple model of the containment flow.

The major contributor to turbulence in the containment following a LOCA is expected to be the steam plume caused by release of the boiling coolant. Although the results shown in section 7 confirm this to be the case, the energy dissipation from the plume is strongly dependent on the details of the accident, and uncertainty in the value of about an order of magnitude should be assumed.

The hydrogen mixing fans and the containment fan coolers are possibly more reliable sources of turbulent energy. They yield values of $\overline{\varepsilon^{1/2}}$ and $\overline{\varepsilon^{3/4}}$ that lie within the range of values found for the steam plume in the three cases considered. Other sources were found not to contribute significantly.

Comparison of the agglomeration mechanisms is shown in figure 3. In the absence of turbulent agglomeration the minimum rate occurs when the particle volume mean radius is $\sim 2\,\mu$m. At the turbulence levels expected in the containment the inertial turbulent agglomeration mechanism does not contribute significantly. For the particular accident conditions assumed in case 2 for the steam plume, the strain mechanism is predicted to have some effect. The contribution is not dramatic, however, and only increases the average rate by about a factor of 2. Using the value for the more reliable source of the hydrogen mixing fans would give a negligible contribution from turbulent agglomeration.

On the basis of the cases considered here, therefore, turbulent agglomeration appears unlikely to make a significant contribution to the overall aerosol growth rate. It is emphasized that the estimates of $\overline{\varepsilon^{1/2}}$ and $\overline{\varepsilon^{3/4}}$ reported here are rather crude. However, it must be recognized that even the most sophisticated methods currently available would yield results that were subject to considerable uncertainty, both in the accuracy of the result for given accident conditions, and in the accident conditions that should be assumed. In the most representative case presently available (the LACE containment) sophisticated methods give results within a factor of 2 of the method used here. Therefore, it is considered that the result of more sophisticated methods are unlikely to alter the conclusion reached here.

10. CONCLUSIONS

A method of analysis of aerosol agglomeration has been developed, based on an equation for the rate of change of the total number of particles N (expressed in terms of a rate "contant" ω). The equation for N is obtained by integrating the full integro-differential agglomeration equation over all particle sizes. The integration loses information on the change in shape of the particle size distribution, $f(R)$, with time, but makes the problem tractable analytically. The approach is useful provided that this ignorance of $f(R)$ does not preclude a calculation of ω. The effect on ω of uncertainties in $f(R)$ has been examined for Brownian, turbulent and gravitational agglomeration mechanisms, with the following results:

For **Brownian** agglomeration, ω is independent of $f(R)$ when the volume mean radius is chosen as the characteristic radius of the distribution (within Smoluchowski's approximation of the Brownian agglomeration kernel).
For **turbulent strain** agglomeration, changes in $f(R)$ change ω by at most a factor of 4. For the range of size distributions that is likely to occur in practice, ω is uncertain to within a factor of 2.
For **gravitational** and **turbulent inertial** agglomeration, the effect of $f(R)$ on ω is theoretically unbounded, since a monodisperse distribution gives no agglomeration, and other distributions do allow agglomeration. However, for the range of size distributions that is likely to occur in practice, ω is again uncertain to within only a factor of 2.

Thus, the rate "constant", ω, can be calculated approximately when the particle size distribution is unknown.

Although the *shape* of the size distribution has only a relatively small effect, the rate of Brownian, gravitational or turbulent inertial agglomeration does depend on the average size of the aerosol particles. The volume mean radius, r_v, can be calculated directly from the total number of particles, N, and the volume fraction, ϕ. Hence, knowledge of the time dependence of N allows the time dependence of r_v to be obtained, either when aerosol deposition rates are negligible (so ϕ is constant) or when the time dependence of ϕ is known.

Turbulent agglomeration has been reviewed. Subsequent experiments support Saffman & Turner's (1956) analysis of turbulent agglomeration, including their suggestion that the turbulent strain collision efficiency $\simeq 1$. The equivalence of turbulent inertial and gravitational agglomeration mechanisms suggests that the turbulent inertial collision efficiency will be the same as the gravitational collision efficiency, which is $\ll 1$.

The analytical approach developed in this paper has been applied to the behaviour of a water aerosol produced in the containment of a PWR by a LOCA. By comparing the rate constants for the various mechanisms, the importance of turbulent agglomeration has been assessed without the need for any assumptions about the aerosol volume fraction, or its size distribution, $f(R)$. It is concluded that:

1. On the basis of the cases considered here, turbulent agglomeration appears unlikely to make a significant contribution to the overall aerosol growth rate. When the mean particle size is less than $\sim 2\,\mu$m, agglomeration is largely due to Brownian motion. When the mean particle size is larger than $\sim 2\,\mu$m, agglomeration is largely due to gravity.
2. The greatest uncertainty in the assessment is in the input data to the containment flow model, which are strongly dependent on the details of the accident. Values have been calculated for specific assumed accidents that are thought to represent the likely range of turbulence conditions.
3. A major difficulty in the calculation of the turbulent agglomeration rate lies in the evaluation of the rate and spatial distribution of dissipation of turbulent energy. In this paper, a simplified model of flow in the containment has been set up and solved to obtain the information necessary to the prediction of turbulent agglomeration rate.
4. The use of more sophisticated containment flow models is unlikely to alter conclusion 1, because (a) the uncertainty in the accident situation would remain and (b) the results of the simple model substantially agree with the results of a more sophisticated model where these are available.

Acknowledgement—This work was carried out at Berkeley Nuclear Laboratories and is published with the permission of Nuclear Electric plc.

REFERENCES

ABRAMOWITZ, M & STEGUN, I. A. 1965 *Handbook of Mathematical Functions.* Dover, New York.

AITCHISON, J. & BROWN, J. A. C. 1973 *The Lognormal Distribution.* Cambridge Univ. Press, U.K.

BATCHELOR, G. K. 1951 Pressure fluctuations in isotropic turbulence. *Proc. Camb. Phil. Soc.* **47,** 359–374.

BRADSHAW, P. 1971 *An Introduction to Turbulence and its Measurement.* Pergamon Press, Oxford.

BRIGGS, G. A. 1975 Plume rise predictions. Presented at the *American Meteorological Society Wkshp on Meteorology and Environment Assessment,* Boston, MA.

DELICHATSIOS, M. A. & PROBSTEIN, R. F. 1975 Coagulation in turbulent flow: theory and experiment. *J. Colloid Interface Sci.* **51,** 394–405.

DUNBAR, I. H. & RAMSDALE, S. A. 1984 Presented at the *CSNI Mtg on Nuclear Aerosols in Reactor Safety,* Karlsruhe, Germany.

FRIEDLANDER, S. K. & WANG, G. S. 1966 The self-preserving particle size distribution for coagulating by Brownian motion. *J. Colloid Interface Sci.* **22,** 126–132.

GITTUS, J. H., ASHWORTH, F. P. O., BILLINGTON, D. E. & BUTTERY, N. E. 1984 Report PWR/R891 Appendix 3F: equipment survival under degraded core conditions.

OKUYAMA, K., KOUSAKA, Y. & YOSHIDA, T. 1978 Turbulent coagulation of aerosols in a pipe flow. *J. Aerosol. Sci.* **9,** 399–410.

PAYNE, J. F. B. 1988 A note on the rate of turbulent strain agglomeration of an aerosol. CEGB Report TPRD/B/PC/0362/M88.

PRESS, W. H., FLANNERY, B. P., TEUKOLSKY, S. A. & VETTERLING, W. T. 1986 *Numerical Recipes, the Art of Scientific Computing.* Cambridge Univ. Press, U.K.

PRUPPACHER, H. R. & KLETT, J. D. 1978 *Microphysics of Clouds and Precipitation.* Reidel, New York.

SAFFMAN, P. G. 1988 Corrigendum to "On the collision of drops in turbulent clouds". *J. Fluid Mech.* **196,** 599.

SAFFMAN, P. G. & TURNER, J. S. 1956 On the collision of drops in turbulent clouds. *J. Fluid Mech.* **1,** 16–30.

SIMONS, S., WILLIAMS, M. M. R. & CASSELL, J. S. 1986 A kernel for combined Brownian and gravitational coagulation. *J. Aerosol Sci.* **17,** 789–793.

SIZEWELL B PRE-CONSTRUCTION SAFETY REPORT 1982. NNC Limited, U.K.

TOWNSEND, A. A. 1976 *The Structure of Turbulent Shear Flow.* Cambridge Univ. Press, U.K.

APPENDIX A

Size Distribution Produced by Brownian Agglomeration

The size distribution resulting from agglomeration obviously depends on the initial size distribution. However, Wang (1966) argues that, at long times, the size distribution approximates to a form that is independent of the initial distribution, namely

$$n^*(V, t) = \frac{N(t)^2}{\phi} \exp\left(-\frac{N(t)V}{\phi}\right),$$

where $n^*(V, t)\,\mathrm{d}V$ is the number of particles per unit volume with volume between V and $V + \mathrm{d}V$. This distribution will now be rewritten as a function of particle radius, $n(r)\,\mathrm{d}r$, i.e. the number of particles per unit volume with a radius between r and $r + \mathrm{d}r$. This is a more convenient form for calculation of agglomeration rates.

Define V_c by $NV_c = \phi$ so that

$$n^*(V, t)\,\mathrm{d}V = \frac{N}{V_c} \exp\left(-\frac{V}{V_c}\right) \mathrm{d}V$$

is the number of particles per unit volume with volume between V and $V + \mathrm{d}V$ and is also the number of particles per unit volume with radius between r and $r + \mathrm{d}r$ provided $(4/3)\pi r^3 = V$ and

$4\pi r^2\,\mathrm{d}r = \mathrm{d}V$. Thus,

$$n(r, t)\,\mathrm{d}r = \frac{N}{V_c}\exp\left(-\frac{V}{V_c}\right)\mathrm{d}V = \frac{3N}{r_c^3}\exp\left(-\frac{r^3}{r_c^3}\right)r^2\,\mathrm{d}r,$$

where r_c is given by $(4/3)\pi r_c^3 = V_c$.

In terms of the dimensionless functions of dimensionless radius, $f(R)$:

$$n(r)\,\mathrm{d}r = \frac{3N}{r_c^3}\exp\left(-\frac{r^3}{r_c^3}\right)r^2\,\mathrm{d}r = N\exp(-R^3)3R^2\,\mathrm{d}R = Nf(R)\mathrm{d}R$$

so

$$f_B(R)\,\mathrm{d}R = \exp(-R^3)3R^2\,\mathrm{d}R,$$

where $f_B(R)\,\mathrm{d}R$ is the dimensionless size distribution for the size distribution generated, at large times, by Brownian agglomeration.

APPENDIX B

Containment Flow Modelling

The model

The model of the containment flow given here is set up for the specific purpose of estimating the energy dissipation within the containment. This limited objective allows one to make simplifying assumptions that render the problem tractable. The most important assumption is that the flow in the containment may be described as one or more jets or plumes which behave like free jets/plumes (until they reach the top of the containment building). In other words, the jets/plumes are assumed to be surrounded by stagnant fluid—the interaction with the weak downflow that must occur to balance the upflow in the jet and the interaction between jets (when more than one is present) are assumed to be negligible. The consequences of this assumption will be considered in the discussion. In all cases, the plumes are assumed to travel 50 m before reaching the top of the containment.

Equations of motion

The equations governing the behaviour of a vertical turbulent buoyant plume in a stagnant ambient atmosphere of contant density may be derived from conservation of momentum, mass and volume (Briggs 1975). Assuming "top-hat" profiles of velocity and density difference (constant up to radius r, zero beyond this radius) the equations are:

$$\frac{\mathrm{d}}{\mathrm{d}z}(\rho_j u^2 r^2) = r^2\Delta\rho g, \qquad [B.1]$$

$$\frac{\mathrm{d}}{\mathrm{d}z}(\rho_j u r^2) = 2ru_e\rho_a \qquad [B.2]$$

and

$$\frac{\mathrm{d}}{\mathrm{d}z}(ur^2) = 2ru_e, \qquad [B.3]$$

where

ρ_j = jet density,
ρ_a = density of the ambient fluid,
$\Delta\rho = \rho_a - \rho_j$,
r = jet radius,
u = jet velocity,
z = vertical distance (positive upwards),
g = acceleration due to gravity

and

u_e = entrainment velocity, effectively defined by [B.3].

Note that a jet is just a special case of a plume with $\rho_j = \rho_a$.

It follows immediately from [B.2] and [B.3] that

$$\frac{d}{dz}(\Delta\rho u r^2) = 0, \qquad [B.4]$$

i.e. the "buoyancy flux" $\Delta\rho u r^2$ is a conserved quantity in the plume.

The equations are incomplete because u_e is not specified. For jets of the same density as the ambient field, dimensional arguments show that u_e scales on u, and experiments show that $u_e \simeq 0.08u$. For a buoyant plume, experiments suggest that $u_e \simeq 0.124u$. The equation

$$u_e = \alpha u \qquad [B.5]$$

is used to determine u_e, with a suitable value for α according as the flow is a jet or a plume. Equations [B.1]–[B.3] and [B.5] can be rearranged to give explicit equations for the variation of r, u and $\Delta\rho$ with z:

$$\frac{du}{dz} = \frac{\left(\frac{g\Delta\rho}{u} - \frac{2\rho_a \alpha u}{r}\right)}{(\rho_a - \Delta\rho)}, \qquad [B.6]$$

$$\frac{dr}{dz} = \alpha - \frac{r}{2u}\frac{du}{dz} \qquad [B.7]$$

and

$$\frac{d}{dz}(\Delta\rho) = -2\alpha\frac{\Delta\rho}{r}. \qquad [B.8]$$

This system of differential equations was solved numerically by the Bulirsch–Stoer method (Press *et al.* 1986). It is only necessary to solve [B.6] and [B.7] for u and r because $\Delta\rho$ is determined by buoyancy flux conservation. However, $\Delta\rho$ was obtained by solving equation [B.8]. This was done to check:

the algebra leading to [B.6]–[B.8],
that the correct equations were programmed into the solver

and

that the equations were solved accurately;

by verifying that the computed values conserve buoyancy flux.

Energy dissipation

The energy dissipated in a horizontal slice of the plume is given by the difference between the kinetic energy fluxes into and out of the slice added to the work done on the slice by pressure forces (the pressure is not constant in a buoyant plume because of the density difference between the plume and ambient fluid, consequently the pressure forces do net work on the plume). Since there are no fixed surfaces, viscous and turbulent stresses at the plume edge must act to increase the momentum of the fluid surrounding the plume. Moving fluid is considered to be part of the plume, so in this simplified model these stresses need not be considered explicitly. Using the top-hat profile approximation again, the energy disspation per unit volume in the plume, at a given downstream distance, is given by

$$\varepsilon\rho_j = -\frac{1}{r^2}\frac{d}{dz}\left(\frac{r^2\rho_j u^3}{2}\right) + ug\Delta\rho. \qquad [B.9]$$

The first term on the right of this equation represents the rate of change of the plume kinetic energy flux with distance, and the second term represents the work done by the buoyancy force. Using

[B.1] and [B.6], [B.9] can be simplified to

$$\varepsilon\rho_j = \frac{\rho_a u^3 \alpha}{r}. \qquad [B.10]$$

The calculation of the turbulent agglomeration rate requires values for the integral of different functions of ε over the containment volume. The integrals of the functions of ε over the plume reduce to integrations over z because of the top-hat profile assumption. The integration over z is accomplished by adding one more differential equation to the system and solving by the Bulirsch–Stoer method as before.

Discussion

The most important assumption of the model is that the fluid outside the plume(s)/jet(s) is essentially stagnant. This assumption obviously precludes the possibility of calculating the distribution of energy dissipation outside the jet. However, as the plume rises energy is fed into it at a constant rate by buoyancy forces, causing the energy to be dissipated (relatively) evenly up the plume. When the plume reaches the top of the containment, its energy is all kinetic, and is likely to be dissipated locally. Furthermore, the results of a much more sophisticated turbulent fluid mechanics model applied to the LACE experiment show that the energy dissipation is much higher in the jet than outside it (Hutton in an unpublished work). The jet occupies a fairly small fraction of the containment volume, so the region outside the jet may still contribute significantly to the integral of $\sqrt{\varepsilon}$ over the containment volume, perhaps as much as the jet itself (an upper limit on this could be calculated from the energy flux in the plume at the top of the containment). This contribution will be very difficult to quantify in a PWR containment because of its complicated geometry (subcompartments, internal structures) and lack of symmetry (causing the flow to be fully three-dimensional).

The calculation of free plume behaviour is obviously crude, with its assumption of top-hat profiles, and its use of a semi-empirical entrainment correlation. The behaviour could be calculated more accurately using a turbulent fluid mechanics computer code. However, it does not seem likely that this would dramatically affect the result.

The plumes spread to a maximum radius $\simeq 10$ m compared to the containment radius of ~ 25 m. This suggests that the downflow will be slow and therefore unlikely to have much effect on the plume. However, where more than one plume/jet is present they are likely to interact towards the top of the containment. Again this will lead to the energy being dissipated less evenly, and reduce the average of $\sqrt{\varepsilon}$.